© 2015. Published by The Company of Biologists Ltd | Development (2015) 142, 2888-2893 doi:10.1242/dev.120212

RESEARCH REPORT

STEM CELLS AND REGENERATION

Retinoic acid signaling spatially restricts osteoblasts and controls ray-interray organization during zebrafish fin regeneration

Nicola Blum[1,2] and Gerrit Begemann[1,*]

ABSTRACT

The zebrafish caudal fin consists of repeated units of bony rays separated by soft interray tissue, an organization that must be faithfully re-established during fin regeneration. How and why regenerating rays respect ray-interray boundaries, thus extending only the existing bone, has remained unresolved. Here, we demonstrate that a retinoic acid (RA)-degrading niche is established by Cyp26a1 in the proximal basal epidermal layer that orchestrates ray-interray organization by spatially restricting osteoblasts. Disruption of this niche causes preosteoblasts to ignore ray-interray boundaries and to invade neighboring interrays where they form ectopic bone. Concomitantly, non-osteoblastic blastema cells and regenerating blood vessels spread into the interrays, resulting in overall disruption of ray-interray organization and irreversible inhibition of fin regeneration. The *cyp26a1*-expressing niche plays another important role during subsequent regenerative outgrowth, where it facilitates the Shha-promoted proliferation of osteoblasts. Finally, we show that the previously observed distal shift of ray bifurcations in regenerating fins upon RA treatment or amputation close to the bifurcation can be explained by inappropriate preosteoblast alignment and does not necessarily require putative changes in proximodistal information. Our findings uncover a mechanism regulating preosteoblast alignment and maintenance of ray-interray boundaries during fin regeneration.

KEY WORDS: Cyp26a1, Caudal fin, Zebrafish, Regeneration, Osteoblast, Interray

INTRODUCTION

Zebrafish regenerate amputated fins by establishing lineage-restricted blastema cells (Gemberling et al., 2013; Tanaka and Reddien, 2011). The zebrafish caudal fin possesses 16-18 fin rays, each consisting of two segmented and opposing hemirays of acellular bone that surround a core of fibroblasts, osteoblasts, pigment cells, arterial blood vessels and nerves (Fig. 1A) (Akimenko et al., 2003). Fin rays are separated by boneless interray tissue, composed of fibroblasts, venous blood vessels, pigment cells and nerves. The principles that compel regenerating fin rays to respect ray-interray boundaries, therefore confining regenerating bone to extend the existing rays, are still unknown. Upon fin amputation, osteoblasts that cover the hemiray surfaces dedifferentiate into proliferating preosteoblasts and migrate into the nascent blastema, where they align at proximal lateral positions (Knopf et al., 2011; Sousa et al., 2011; Stewart and Stankunas, 2012). Thus, preosteoblasts form a layer between the basal epidermal layer and fibroblast-derived blastema cells. The distal blastema remains devoid of preosteoblasts. During subsequent regenerative outgrowth, proliferating preosteoblasts at the distal leading edge become differentiating osteoblasts in more proximal parts (Stewart et al., 2014). Notably, neither osteoblasts nor non-osteoblastic blastema cells mix with adjacent interray cells (Stewart and Stankunas, 2012). Thus, the regenerating fin consists of repeating blastema units dedicated to each fin ray that are separated by regenerating interrays (Fig. 1A).

[1]Developmental Biology, University of Bayreuth, Bayreuth 95440, Germany. [2]RTG1331, Department of Biology, University of Konstanz, Konstanz 78457, Germany.

*Author for correspondence (gerrit.begemann@uni-bayreuth.de)

Received 23 November 2014; Accepted 22 July 2015

RESULTS AND DISCUSSION

cyp26a1-expressing epidermal niches control preosteoblast alignment and ray-interray organization

During fin regeneration, fin rays respect ray-interray boundaries. An interesting exception occurs after amputation close to a bifurcation site (short cut, Fig. 1B). In such regenerates, sister rays ignore ray-interray boundaries and fuse (Fig. 1C) (Laforest et al., 1998), whereby the probability for ray fusion increases as the distance between them decreases (Fig. 1D). Using the *osc:gfp* line, which allows detection of preosteoblasts in the early blastema (Knopf et al., 2011; Sousa et al., 2011), we found ectopic preosteoblasts in the interray separating the two sister rays at 2 dpa (Fig. 1E). This finding reveals that sister ray fusion is due to preosteoblasts spreading into the interray. We were interested in the mechanisms that cause preosteoblasts to respect ray-interray boundaries. *shha* is expressed within the basal epidermal layer adjacent to pre- and differentiating osteoblasts (supplementary material Fig. S1) (Laforest et al., 1998; Lee et al., 2009; Quint et al., 2002; Zhang et al., 2012). We found a similar expression pattern for the RA-degrading enzyme *cyp26a1* (Fig. 1F,G). By contrast, the RA-synthesizing enzyme *aldh1a2* is expressed in fibroblast-derived blastema cells (Fig. 1G) (Blum and Begemann, 2012). Although proximal fibroblast-derived blastema cells express *cyp26b1* (Blum and Begemann, 2015), it is unlikely that RA diffusion into adjacent epidermal cells is efficiently prevented. We thus suspected that *cyp26a1*-expressing cells provide niches of low RA levels that might facilitate expression of RA-sensitive genes.

It has been shown that immersion of fish in RA reduces *shha* expression (Laforest et al., 1998). However, RA administration via immersion induces epidermal cell death (Ferretti and Géraudie, 1995; Géraudie and Ferretti, 1997); therefore, it has remained unclear whether this was a specific effect. We used intraperitoneal (IP) injection of RA, which efficiently enhances RA levels in the adult fin without causing cell death (Blum and Begemann, 2012), and found decreased expression of *shha* and of the Hh receptor and target *ptch2* 6 h after injection at 4 dpa (Fig. 1H). Injection of R115866, a selective antagonist of Cyp26 enzymes (Hernandez et al., 2007; Stoppie et al., 2000), also caused downregulation of *shha* and *ptch2* (Fig. 1H,I), indicating that *shha* expression requires RA degradation. Accordingly, overexpression of *cyp26a1* in *hsp70l:*

Development (2015) 142, 2888-2893 doi:10.1242/dev.120212

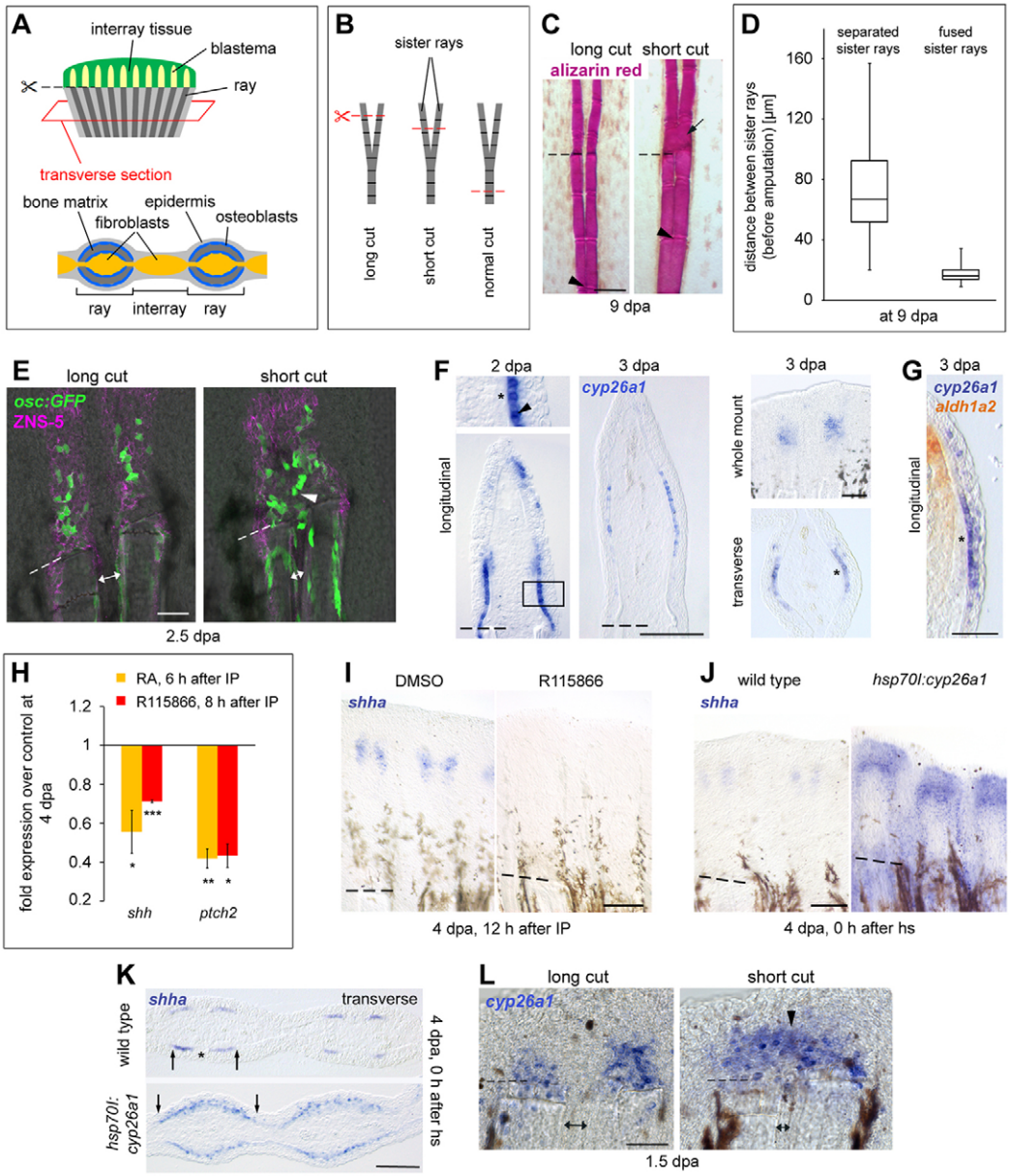

Fig. 1. *shha* expression is controlled by *cyp26a1*-expressing epidermal niches. Lateral expansion of the *cyp26a1*-expressing niches and misguidance of preosteoblasts precede fusion of sister rays. (A) Overview of a regenerating fin. (B) Schematized representation of the amputation levels. (C-E,L) Amputations in proximity to bifurcations cause fusion of *cyp26a1* expression domains (arrowhead in L), followed by spreading of preosteoblasts into the interray separating the two sister rays (arrowhead in E) and fusion of sister rays (arrow in C). (C) Alizarin Red staining at 9 dpa. Arrowheads indicate branching sites. (D) Distance range between sister rays for separated and fused rays. (E) IHC for ZNS-5 and GFP in *osc:gfp* fish at 2.5 dpa. (F,G) WISH and ISH on sections for *cyp26a1* reveals expression in the proximal basal epidermal layer (arrowhead) adjacent to preosteoblasts (asterisks) at 2 and 3 dpa. (G) *aldh1a2* is expressed in fibroblast-derived blastema cells, but not in preosteoblasts adjacent to *cyp26a1*-expressing cells. (H,I) RA and R115866 injection downregulates *shha* and *ptch2*. Transcript levels 6 or 8 hours after injection at 4 dpa measured by qPCR (H); WISH for *shha* 12 hours after R115866 injection at 4 dpa (I). (J,K) Overexpression of *cyp26a1* in *hsp70l:cyp26a1* fish at 4 dpa causes upregulation of *shha* expression and lateral expansion of the expression domains. Arrows mark the lateral expression limits. Of note, *shha* in wild-type controls is already expressed in subdomains due to the upcoming bifurcation event. (L) WISH for *cyp26a1* at 1.5 dpa. Double-headed arrows in E and L: distance between sister rays. Asterisk marks the gap between the two subdomains. Data are represented as mean±s.e.m. **P*<0.05, ***P*<0.01, ****P*<0.001. Dashed lines indicate amputation plane. Scale bars: 100 µm. h, hours; hs, heat shock.

cyp26a1 fish (Blum and Begemann, 2012) at 4 dpa resulted in enhanced and laterally extended *shha* expression within the basal epidermal layer directly at the end of a single heat shock (Fig. 1J,K). We did not observe *shha* expression in interrays. We propose that this was due to the requirement for Fgfs (and putative other blastema-derived signals) for *shha* expression (Lee et al., 2009).

Short-cut amputations resulted in shared *cyp26a1* expression domains between sister rays at 1.5 dpa (Fig. 1L), indicating that fusion of the RA-degrading niches precedes spreading of preosteoblasts into interrays. To examine how preosteoblasts behave if efficient lowering of RA levels in the *cyp26a1*-niches fails, we injected fish with RA or R115866, starting with the first IP directly after amputation (normal cut). We observed spreading of preosteoblasts into interrays in RA- and R115866-injected *osc:gfp* fish at 2.5 dpa (Fig. 2A; data not shown), indicating that preosteoblasts failed to align at proximolateral parts of the

Development (2015) 142, 2888-2893 doi:10.1242/dev.120212

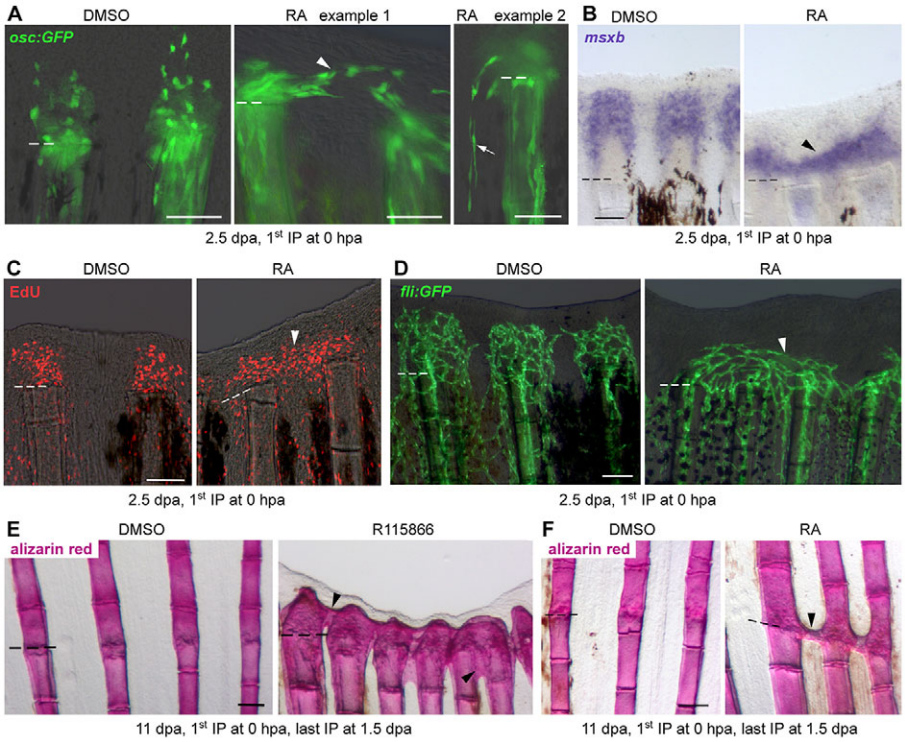

Fig. 2. Preosteoblast alignment and maintenance of the ray-interray organization requires RA-degrading epidermal niches. (A) IHC for GFP in *osc:gfp* fish reveals ectopic GFP$^+$ preosteoblasts in interrays in RA-treated fish at 2.5 dpa. Arrowhead indicates preosteoblast in interray tissue, arrow indicates proximally migrating preosteoblast in interray tissue. (B,C) WISH for *msxb* (B) and EdU labeling (C) at 2.5 dpa demonstrate expansion of blastema cells into interrays in RA-treated fish. Arrowheads indicate ectopic blastema cells. (D) *fli:gfp* fish show misconnected blood vessels (arrowhead) in RA-treated fish at 2.5 dpa. (E,F) RA and R115866 treatment during blastema formation result in formation of ectopic bone at the wound site and in R115866-treated fish in an irreversible regeneration block. Arrowheads indicate ectopic bone, dashed lines indicate amputation plane. Scale bars: 100 µm.

blastema and disregarded ray-interray boundaries. Of note, formation of a distinct basal epidermal layer was not inhibited (supplementary material Fig. S2A). As R115866 treatment also reduced Cyp26b1 activity in fibroblast-derived blastema cells, we cannot exclude that misguidance of preosteoblasts in R115866- or RA-treated fish was at least partially due to enhanced RA levels in the mesenchyme. However, the expression pattern of *cyp26a1* strongly supports a model in which alignment, and thereby spatial restriction of preosteoblasts, is controlled by signals from *cyp26a1*-expressing epidermal cells.

Interestingly, treatment with RA or R115866 also caused expansion of the blastema marker *msxb* (Akimenko et al., 1995) into interrays (Fig. 2B; supplementary material Fig. S2B). 5-ethynyl-2′-deoxyuridine (EdU) labeling further suggested that these were cycling blastema cells (Fig. 2C). We did not observe an enlarged preosteoblast or *msxb*$^+$ cell population in RA- or R115866-treated fish (Fig. 2A,B; supplementary material Fig. S2B), thus making it unlikely that spreading into interrays was simply due to increased cell numbers.

Blood vessels regenerate into the blastema accompanied by anastomosis between the injured arteries and veins of the same ray (Huang et al., 2003). Intriguingly, wounded arteries and veins had formed connections with vessels of neighboring rays in RA- and R115866-treated *fli:gfp* fish (Lawson and Weinstein, 2002) at 2.5 dpa (Fig. 2D; data not shown). Together, these data show that also non-osteoblastic cell types ignore ray-interray boundaries if efficient RA degradation in the proximal basal epidermal layer fails.

Expansion of *msxb* expression into interrays was also observed in regenerates that lacked preosteoblasts, but showed expression of *cyp26a1* (supplementary material Fig. S3). This was achieved by treating fish with the Hh inhibitor cyclopamine from 24 hpa onwards, a treatment condition that is expected to inhibit preosteoblast proliferation in the stump. We thus conclude that, rather than signals from *cyp26a1*-expressing cells, aligning preosteoblasts themselves provide spatial orientation for non-osteoblastic blastema cells.

To test how disrespect of ray-interray boundaries by blastema cells affects the overall organization of the regenerating fin, we gave the last RA or R115866 injection at 1.5 dpa and examined the long-term consequences for regeneration. Of note, owing to autoregulatory feedback mechanisms of RA signaling, *cyp26a1* expression became upregulated in the entire regenerate during RA or R115866 treatment (data not shown). This upregulation can only counterbalance small fluctuations in RA levels and can therefore be neglected during the treatment period. However, ectopic expression persisted for some days after termination of treatment (supplementary material Fig. S4A), and was therefore expected to allow for *shha* expression in the entire regenerate. Consistently, we detected *shha* expression in both rays and interrays in R115866-treated *shh:gfp* fish (Ertzer et al., 2007) 2 days after treatment was stopped at 4 dpa (supplementary data Fig. S4B). As heat shock-induced overexpression of *cyp26a1* at 4 dpa is insufficient to induce *shha* expression in interrays (Fig. 1J,K), this result suggests that *shha* expression in interrays in R115866-treated fish was due to ectopic blastema cells in the interray region. Thus, this finding supports a model in which *shha* expression is spatially confined by RA-degrading epidermal cells and signals from underlying blastema cells.

In fins of R115866-treated fish, regeneration was subsequently irreversibly blocked and ectopic bone had formed in interrays at 11 dpa (Fig. 2E). However, bone matrix did not seal the wound (supplementary material Fig. S5), indicating that inhibition of regeneration was not due to a mechanical block but rather due to mispatterning of the early regenerate. In RA-treated fins, neighboring rays were occasionally connected by bony bridges at the amputation site (Fig. 2F), but otherwise, regeneration proceeded normally. This weaker phenotype was probably due to rapid clearance of excess RA after treatment had stopped. When fins were amputated within the third segment distal to the first branching point (long cut), RA treatment caused fusions of sister rays (supplementary material Fig. S6A). This is consistent with results

Development (2015) 142, 2888-2893 doi:10.1242/dev.120212

obtained previously by RA treatment via immersion (Géraudie and Ferretti, 1997; Géraudie et al., 1995; White et al., 1994). We next determined the distance range at which formation of ectopic bone occurs, and found a much greater range in RA-treated fish (supplementary material Fig. S6B). Fusion of sister rays had sometimes been interpreted as a proximalization of the regenerate (White et al., 1994). However, our data show that sister rays fuse if preosteoblasts spread into interrays, which can be caused either by insufficient lowering of RA levels in the proximal basal epidermal layer or by induction of two RA-degrading domains in close proximity. Thus, our findings provide a more parsimonious explanation for sister ray fusion that is not based on putative changes in proximodistal information.

Cyp26a1 activity facilitates osteoblast proliferation through *shha* expression

Proliferation of preosteoblasts has been suggested to be controlled by Shha (Laforest et al., 1998; Lee et al., 2009; Quint et al., 2002; Zhang et al., 2012). We found reduced osteoblast proliferation within 12 h of cyclopamine treatment (Fig. 3A). Osteoblast differentiation was unaffected (supplementary data Fig. S7). Moreover, we did not detect TUNEL^{+} osteoblasts in control or cyclopamine-treated fish (data not shown). Hence, even though RA signaling promotes osteoblast proliferation (Blum and Begemann, 2015), prolonged experimental RA exposure should cause downregulation of *shha* and consequently lead to a reduction of osteoblast proliferation. Indeed, osteoblast proliferation was reduced 12 h after RA injection at 3 dpa (Fig. 3B). Neither osteoblasts nor other cells undergo cell death after RA treatment via IP injections (Blum and Begemann, 2012). Concomitant activation of Hh signaling, using the Smoothened agonist SAG, rescued osteoblast proliferation (Fig. 3C), thus confirming that decreased proliferation upon RA treatment was due to impaired Hh signaling. Together, these findings indicate that Shha from *cyp26a1*-expressing epidermal cells promotes proliferation of adjacent osteoblasts. Interestingly, cyclopamine treatment has been reported to block proliferation of fibroblast-derived blastema cells (Lee et al., 2009), for which *ptch* expression has not been demonstrated. Accordingly, prolonged RA treatment downregulated proliferation of fibroblast-derived blastema cells, and concomitant SAG treatment could rescue this effect (supplementary material Fig. S8). Although we cannot exclude a direct effect, Hh signaling might indirectly promote proliferation of other cell types via osteoblasts.

Besides a requirement for *shha* expression, Fgf signaling has been shown to exclude *shha* from distal regions (Lee et al., 2009), suggesting that Fgf signaling restricts *shha* to the proximal basal epidermal layer by repressing *cyp26a1*. We manipulated Fgf signaling at 3 dpa by either overexpressing a dominant negative Fgfr1 (*hsp70l:dn-fgfr1*; Lee et al., 2005) or a constitutively active Ras (*hsp70l:v-ras*; Lee et al., 2009) and quantified *cyp26a1* expression. *cyp26a1* was downregulated in *hsp70l:v-ras* fish 2 h after a single heat shock and upregulated in *hsp70l:dn-fgfr1* fish at the end of a single heat shock (Fig. 3D), demonstrating that Fgf signaling inhibits *cyp26a1* expression. Thus, proximal expansion of Fgf signaling should result in proximal regression of *cyp26a1* expression. We took advantage of the finding that Fgf activity expands more proximally in fins that had been amputated at a more proximal position and retracts distally as regeneration proceeds

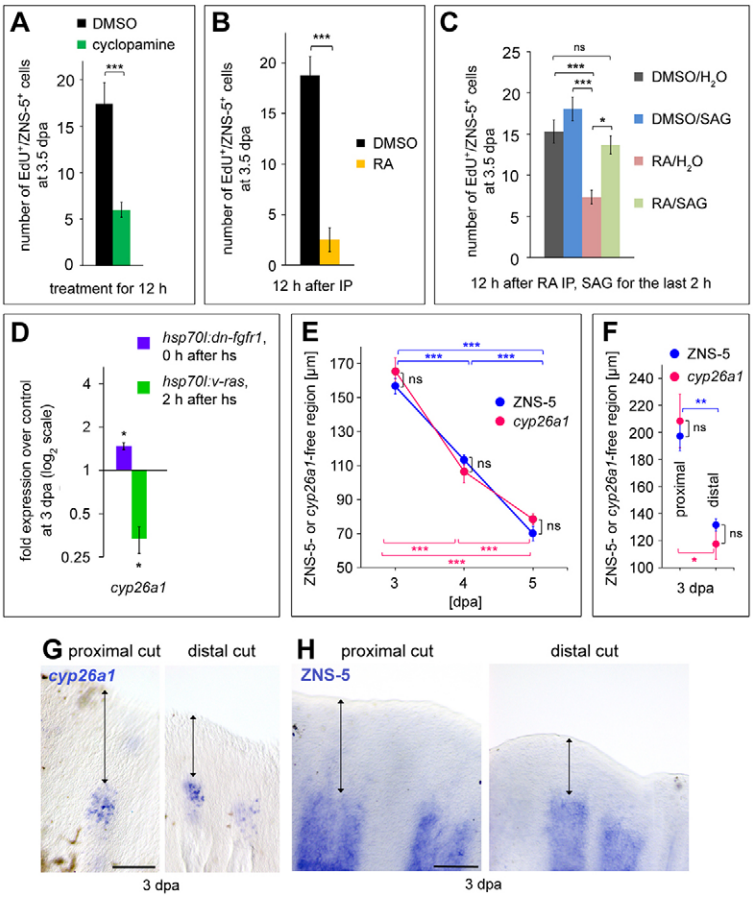

Fig. 3. Shha-promoted osteoblast proliferation requires *cyp26a1* expression that is restricted to proximal regions by Fgf activity. (A,B) Cyclopamine (A) or prolonged RA (B) treatment downregulates osteoblast proliferation. EdU^{+}/ZNS-5^{+} cells per section at 3.5 dpa. (C) Inhibition of osteoblast proliferation 12 h after RA injection can be rescued by concomitant SAG treatment. EdU^{+}/ZNS-5^{+} cells per section at 3.5 dpa. (D) Inhibition of Fgf signaling in *hsp70l:dn-fgfr1* fish results in upregulation of *cyp26a1* expression. Conversely, activation of Fgf signaling in *hsp70l:v-ras* fish results in the downregulation of *cyp26a1*. Transcript levels at 3 dpa measured by qPCR. (E-H) ZNS-5- and *cyp26a1*-free distal domains (double-headed arrows) extend further proximally in regenerates that had been amputated at a more proximal level at 3 dpa (F-H), and retracts distally as regeneration proceeds (E). (G) WISH for *cyp26a1*. (H) IHC for ZNS-5. (E,F) Length of the *cyp26a1*- or ZNS-5-free distal domain. Data are represented as mean±s.e.m. **P*<0.05, ***P*<0.01, ****P*<0.001. ns, not significant; hs, heat shock. Scale bars: 100 µm.

Development (2015) 142, 2888-2893 doi:10.1242/dev.120212

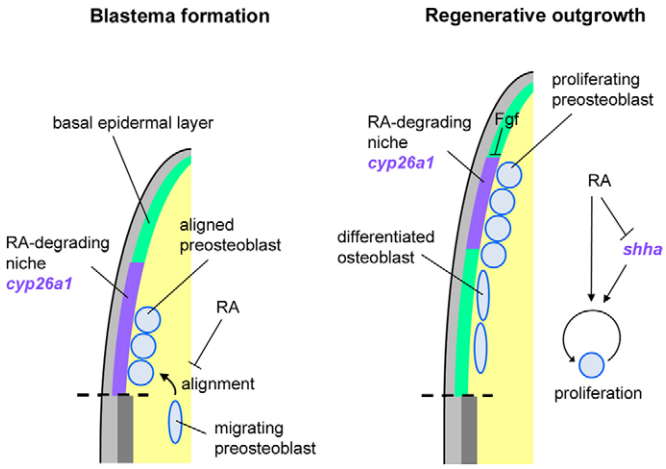

Fig. 4. Model for Cyp26a1 functions during fin regeneration. Schematic summary of Cyp26a1-mediated preosteoblast alignment and proliferation.

(Lee et al., 2005, 2009). We found that amputation at a proximal position results in a proximal shift of the *cyp26a1* expression domain (Fig. 3F,G). In return, *cyp26a1* expression shifted distally during the course of regeneration (Fig. 3E). Notably, also the distal limit of aligned preosteoblasts was always adjacent to the distal limit of *cyp26a1* expression (Fig. 3E-H), suggesting that *cyp26a1*-expressing cells spatially confine preosteoblasts also along the proximodistal axis.

Conclusions

During fin regeneration the ray-interray organization has to be faithfully re-established in order to rebuild an exact copy of the lost fin parts and to ensure proper function of the regenerated fin. Here, we show that disrespect of the ray-interray boundaries by preosteoblasts and other blastema cells in the nascent blastema has adverse consequences for subsequent fin patterning and may disrupt the whole regeneration process. Our findings support a model in which signals from RA-degrading niches established by Cyp26a1 in the basal epidermal layer ensure the appropriate initial alignment of preosteoblasts in the nascent blastema (Fig. 4) and compel blastema cells to respect ray-interray boundaries. Furthermore, during regenerative outgrowth, Cyp26a1 activity remains important to facilitate Shha-promoted proliferation in adjacent preosteoblasts (Fig. 4).

MATERIALS AND METHODS

Zebrafish husbandry, fin amputations, heat shock and drug treatment conditions

Zebrafish were raised under standard conditions at 27-28°C. Caudal fins of 3- to 18-month-old fish were amputated along the dorsoventral axis, intersecting the median rays halfway for normal cuts, at ~30% ray length for proximal cuts, at ~70% for distal cuts, within 1-2 segments distal to the first branching point for short cuts and within the third segment away for long cuts. Heat shocks were performed at 38°C for 1 h. Approximately 20 µl RA (all-trans RA, Sigma) or R115866 (Janssen Pharmaceutica) were intraperitoneally injected into size-matched siblings every 12 h. RA: 1 mM in 1% DMSO/PBS. R115866: 0.67 mM 10% DMSO/PBS. For cyclopamine treatment, fish were incubated in 5 µM cyclopamine (Sigma), 0.1% EtOH, 0.1% DMSO in E3-medium (HEPES-buffered at pH 7.4). Cyclopamine was exchanged daily. SAG (Calbiochem) treatment was performed using 5 µM SAG in E3-medium. SAG stock solution was prepared in water. Control fish were always treated with an equivalent concentration of the drug solvent. All animal experiments were approved by the state of Baden-Württemberg, Germany.

Osteoblast differentiation, qPCR, TUNEL staining, EdU labeling and cryosectioning

Osteoblast differentiation was examined by measuring the GFP-free distal region in *osx:gfp* fish (*Olsp7:nlsgfp*; Spoorendonk et al., 2008). Gene expression levels were analyzed by qPCR (for primers see supplementary material Table S1), cell death by TUNEL staining and cell proliferation by EdU labeling. Cryosectioning was used to produce longitudinal and transverse fin sections. Further information concerning these methods, as well as descriptions of length measurements and cell number quantifications, imaging, immunohistochemistry, *in situ* hybridization and Alizarin Red staining can be found in the supplementary material methods.

Statistics

Student's *t*-test was used to test significance of differences. The numbers of specimens used are given in supplementary material Table S2.

Acknowledgements

We thank S. Schulte-Merker, K. Poss and U. Strähle for transgenic fish lines, Janssen Pharmaceutica for the R115866 compound, and A. Pfeifer, I. Zerenner-Fritsche, S. Leuschner and K.-H. Pöhner for fish care.

Competing interests

The authors declare no competing or financial interests.

Author contributions

N.B. conceived the study, and designed, performed and analyzed experiments. N.B. and G.B. wrote the manuscript.

Funding

N.B. was supported by fellowships from the University of Konstanz and the Research Training Group (RTG) 1331, and by a travelling fellowship from The Company of Biologists. This work was supported by a grant from the Deutsche Forschungsgemeinschaft [BE 1902/6-1 to G.B.].

Supplementary material

Supplementary material available online at
http://dev.biologists.org/lookup/suppl/doi:10.1242/dev.120212/-/DC1

References

Akimenko, M. A., Johnson, S. L., Westerfield, M. and Ekker, M. (1995). Differential induction of four msx homeobox genes during fin development and regeneration in zebrafish. *Development* **121**, 347-357.

Akimenko, M.-A., Marí-Beffa, M., Becerra, J. and Géraudie, J. (2003). Old questions, new tools, and some answers to the mystery of fin regeneration. *Dev. Dyn.* **226**, 190-201.

Blum, N. and Begemann, G. (2012). Retinoic acid signaling controls the formation, proliferation and survival of the blastema during adult zebrafish fin regeneration. *Development* **139**, 107-116.

Blum, N. and Begemann, G. (2015). Osteoblast de- and redifferentiation are controlled by a dynamic response to retinoic acid during zebrafish fin regeneration. *Development* **142**, 2894-2903.

Ertzer, R., Müller, F., Hadzhiev, Y., Rathnam, S., Fischera, N., Rastegara, S. and Strähle, U. (2007). Cooperation of sonic hedgehog enhancers in midline expression. *Dev. Biol.* **301**, 578-589.

Ferretti, P. and Géraudie, J. (1995). Retinoic acid-induced cell death in the wound epidermis of regenerating zebrafish fins. *Dev. Dyn.* **202**, 271-283.

Gemberling, M., Bailey, T. J., Hyde, D. R. and Poss, K. D. (2013). The zebrafish as a model for complex tissue regeneration. *Trends Genet.* **29**, 611-620.

Géraudie, J. and Ferretti, P. (1997). Correlation between RA-induced apoptosis and patterning defects in regenerating fins and limbs. *Int. J. Dev. Biol.* **41**, 529-532.

Géraudie, J., Monnot, M. J., Brulfert, A. and Ferretti, P. (1995). Caudal fin regeneration in wild type and long-fin mutant zebrafish is affected by retinoic acid. *Int. J. Dev. Biol.* **39**, 373-381.

Hernandez, R. E., Putzke, A. P., Myers, J. P., Margaretha, L. and Moens, C. B. (2007). Cyp26 enzymes generate the retinoic acid response pattern necessary for hindbrain development. *Development* **134**, 177-187.

Huang, C.-c., Lawson, N. D., Weinstein, B. M. and Johnson, S. L. (2003). Reg6 is required for branching morphogenesis during blood vessel regeneration in zebrafish caudal fins. *Dev. Biol.* **264**, 263-274.

Knopf, F., Hammond, C., Chekuru, A., Kurth, T., Hans, S., Weber, C. W., Mahatma, G., Fisher, S., Brand, M., Schulte-Merker, S. et al. (2011). Bone regenerates via dedifferentiation of osteoblasts in the zebrafish fin. *Dev. Cell* **20**, 713-724.

Development (2015) 142, 2888-2893 doi:10.1242/dev.120212

Laforest, L., Brown, C. W., Poleo, G., Géraudie, J., Tada, M., Ekker, M. and Akimenko, M. A. (1998). Involvement of the sonic hedgehog, patched 1 and bmp2 genes in patterning of the zebrafish dermal fin rays. *Development* **125**, 4175-4184.

Lawson, N. D. and Weinstein, B. M. (2002). In vivo imaging of embryonic vascular development using transgenic zebrafish. *Dev. Biol.* **248**, 307-318.

Lee, Y., Grill, S., Sanchez, A., Murphy-Ryan, M. and Poss, K. D. (2005). Fgf signaling instructs position-dependent growth rate during zebrafish fin regeneration. *Development* **132**, 5173-5183.

Lee, Y., Hami, D., De Val, S., Kagermeier-Schenk, B., Wills, A. A., Black, B. L., Weidinger, G. and Poss, K. D. (2009). Maintenance of blastemal proliferation by functionally diverse epidermis in regenerating zebrafish fins. *Dev. Biol.* **331**, 270-280.

Quint, E., Smith, A., Avaron, F., Laforest, L., Miles, J., Gaffield, W. and Akimenko, M.-A. (2002). Bone patterning is altered in the regenerating zebrafish caudal fin after ectopic expression of sonic hedgehog and bmp2b or exposure to cyclopamine. *Proc. Natl. Acad. Sci. USA* **99**, 8713-8718.

Sousa, S., Afonso, N., Bensimon-Brito, A., Fonseca, M., Simões, M., Leon, J., Roehl, H., Cancela, M. L. and Jacinto, A. (2011). Differentiated skeletal cells contribute to blastema formation during zebrafish fin regeneration. *Development* **138**, 3897-3905.

Spoorendonk, K. M., Peterson-Maduro, J., Renn, J., Trowe, T., Kranenbarg, S., Winkler, C. and Schulte-Merker, S. (2008). Retinoic acid and Cyp26b1 are critical regulators of osteogenesis in the axial skeleton. *Development* **135**, 3765-3774.

Stewart, S. and Stankunas, K. (2012). Limited dedifferentiation provides replacement tissue during zebrafish fin regeneration. *Dev. Biol.* **365**, 339-349.

Stewart, S., Gomez, A. W., Armstrong, B. E., Henner, A. and Stankunas, K. (2014). Sequential and opposing activities of Wnt and BMP coordinate zebrafish bone regeneration. *Cell Rep.* **6**, 482-498.

Stoppie, P., Borgers, M., Borghgraef, P., Dillen, L., Goossens, J. A. N., Sanz, G., Szel, H., Hove, C. V. A. N., Nyen, G. V. A. N., Nobels, G. et al. (2000). R115866 inhibits all- trans -retinoic acid metabolism and exerts retinoidal effects in rodents. *J. Pharmacol. Exp. Ther.* **293**, 304-312.

Tanaka, E. M. and Reddien, P. W. (2011). The cellular basis for animal regeneration. *Dev. Cell* **21**, 172-185.

White, J. A., Boffa, M. B., Jones, B. and Petkovich, M. (1994). A zebrafish retinoic acid receptor expressed in the regenerating caudal fin. *Development* **120**, 1861-1872.

Zhang, J., Jeradi, S., Strähle, U. and Akimenko, M.-A. (2012). Laser ablation of the sonic hedgehog-a-expressing cells during fin regeneration affects ray branching morphogenesis. *Dev. Biol.* **365**, 424-433.